ally believed to result from gas and liquid expulsion (*11*).
33. C. K. Paull, *Geology* **15**, 545 (1987); R. F. Commeau *et al.*, *Earth Planet. Sci. Lett.* **82**, 62 (1985).
34. M. Rio *et al.*, *Bull. Soc. Géol. France* **8**, 151 (1985).
35. D. Desbruyères *et al.*, *Bull. Biol. Soc. Washington* **6**, 103 (1985).
36. Five pyrite samples from the ERI and PPI mounds yielded $\delta^{34}S$ values ranging from −8.1 to −20.7 per mil CDT (mean = −17.9 per mil), which is in the isotopic range of pyrite derived from bacterial sulphate reduction [H. R. Krouse, *Handbook of Environmental Isotope Geochemistry*, P. Fritz and J. C. Fontes, Eds. (Elsevier, Amsterdam, 1980), pp. 436–471].
37. E. W. Behrens, *Am. Assoc. Petrol. Geol. Bull.* **72**, 105 (1988); M. Hovland and J. H. Sommerville, *Mar. Petrol. Geol.* **2**, 319 (1985).
38. We thank the late J. A. Jeletzky for providing fossil determinations and A. F. Embry, D. Morrow, and two anonymous scientists for critically reviewing the manuscript. This research was supported by Energy, Mines, and Resources, Canada, The Polar Continental Shelf Project, and the Natural Science and Engineering Research Council of Canada.

13 October 1988; accepted 3 February 1989

Dynamics of Liquefaction During the 1987 Superstition Hills, California, Earthquake

T. L. HOLZER, T. L. YOUD, T. C. HANKS

Simultaneous measurements of seismically induced pore-water pressure changes and surface and subsurface accelerations at a site undergoing liquefaction caused by the Superstition Hills, California, earthquake (24 November 1987; M = 6.6) reveal that total pore pressures approached lithostatic conditions, but, unexpectedly, after most of the strong motion ceased. Excess pore pressures were generated once horizontal acceleration exceeded a threshold value.

SEISMICALLY INDUCED LIQUEFACTION involves the loss of static shearing resistance of saturated, relatively loose, sandy deposits due to a tendency to closer packing of the constituent grains dynamically driven by seismic shear waves. If pore fluid in the liquefying layer cannot escape, this reduction in pore volume causes pore-water pressure to increase. Liquefaction is generally thought to occur when pore pressures approach lithostatic. Common surface manifestations of liquefaction include fountains of water laden with sediment and ground failure.

In this paper, we report simultaneous measurements of pore-water pressure change in a natural sand layer and earthquake shaking above and below the layer while it underwent liquefaction during the moment magnitude M = 6.6 (*1*) Superstition Hills earthquake (0515 PST, 24 November 1987). We also have such records for the preceding Elmore Ranch earthquake (1754 PST, 23 November 1987; M = 6.2) and aftershocks to each of these events (Table 1), none of which generated excess pore pressure. Understanding of liquefaction has been based primarily on laboratory investigations and post-earthquake field investigations (*2*). A few earlier measurements of pore pressure in loose sands during earthquakes have been made but not of the buildup of pore pressure to a lithostatic condition (*3*).

The engineering significance of liquefaction potential is enormous because many of the world's major cities are partly built upon young, saturated sediments. Understanding the mechanisms of liquefaction is also important in paleoseismology, because sand boils preserved in the geologic record have been used to date and to estimate magnitudes of prehistoric earthquakes (*4*). In the eastern United States, for example, ancient sand boils are the only reliable indicator of prehistoric earthquakes, in that surface fault scarps are absent—or, perhaps, have not yet been found—in this large region (*5*).

Our data come from an array of instruments deployed on and beneath the floodplain of the Alamo River in the Imperial Valley, California, a desert area that is heavily irrigated for crop cultivation (Fig. 1A). This site is 23 km east of the epicenter of the Elmore Ranch earthquake and 31 km east-northeast of the epicenter of the Superstition Hills earthquake. Our attention was drawn to the site when it experienced liquefaction during the Westmorland earthquake (26 April 1981; M = 5.9) (Fig. 1A). Instrumentation was installed in 1982 (*6*).

Shallow deposits at the array consist of saturated, floodplain sediments that fill an old incised channel of the Alamo River (*7*). The deposits probably date from catastrophic flooding of the river between 1905 and 1907 (*8*). The uppermost unit at the array is a 2.5-m-thick flat-lying silt bed that overlies the unit that liquefied, a 4.5-m-thick silty sand (Fig. 1B). The fines content (<75 μm) of the silty sand averages 33% and ranges from 16 to 60%; porosity is about 41%. Beneath these floodplain deposits is a 5-m-thick silty clay unit, the uppermost unit of a dense and regionally extensive sedimentary deposit. The Alamo River, a perennial stream because of drainage from irrigation, currently occupies a 3.7-m-deep channel 23 m east of the center of the array and controls the water table depth at about 1.2 m. Despite the shallow water table, the land surface usually is arid because of the desert conditions.

Six pore-water pressure transducers and two three-component force-balance acceler-

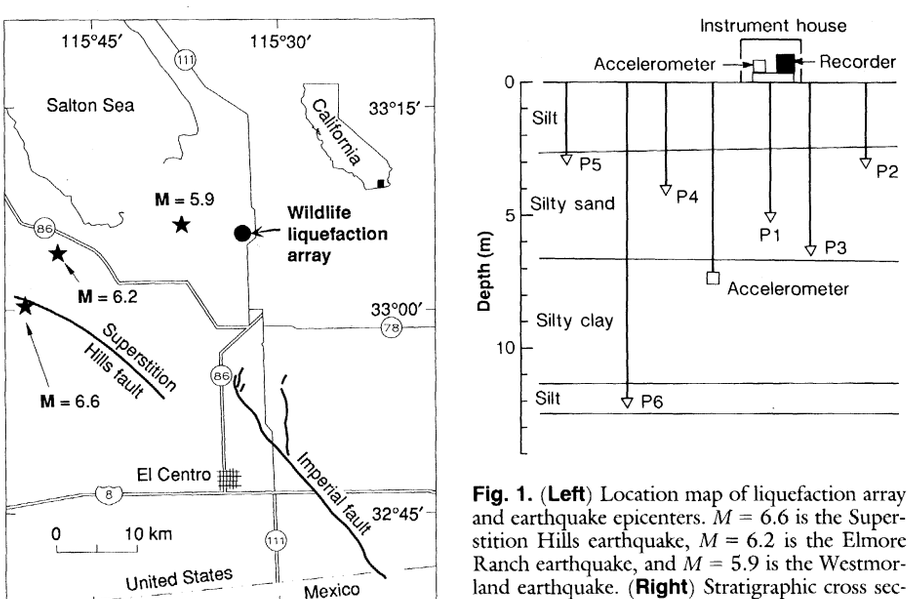

Fig. 1. (**Left**) Location map of liquefaction array and earthquake epicenters. M = 6.6 is the Superstition Hills earthquake, M = 6.2 is the Elmore Ranch earthquake, and M = 5.9 is the Westmorland earthquake. (**Right**) Stratigraphic cross section of array and schematic of instrument deployment. In plan view, pore-pressure transducers (denoted by P) are equally spaced on the perimeter of a circle with a diameter of 9.1 m. Accelerometers are near center of circle (*7*).

T. L. Holzer and T. C. Hanks, U.S. Geological Survey, 345 Middlefield Road, Menlo Park, CA 94025.
T. L. Youd, Department of Civil Engineering, Brigham Young University, Provo, UT 84602.

ometers, one at the surface and one downhole, are installed at the array (Fig. 1B). In addition, an inclinometer casing, to detect permanent lateral subsurface deformation, extends to a depth of 8.8 m. Five of the pore-pressure transducers are in the liquefiable, silty sand layer at depths ranging from 2.9 to 6.6 m; the sixth is at a depth of 12 m, in a dense, 1-m-thick, silt layer well beneath the liquefiable layer (*9*). The downhole accelerometer is at a depth of 7.5 m, beneath the liquefiable silty sand. The shear-wave travel time across the separation between the downhole and surface accelerometers is, on the basis of in situ measurements of shear-wave velocity (*10*), 0.06 s. All 12 channels of data are recorded on the same analogue recording device, which is set to trigger on 0.01g of vertical ground acceleration and to continue recording for 60 s following the last acceleration of 0.01g.

Liquefaction of the silty sand layer during the Superstition Hills earthquake caused sand boils to erupt water and muddy sediment and turned the otherwise arid array site into a quagmire. Even so, the total volume of water and sediment that discharged to the surface probably amounted to less than 1% of the total thickness of the liquefied layer. The volume could be estimated because the discharged material ponded at the array. The aggregate area in the floodplain affected by liquefaction equaled about 33 ha.

Extensive ground cracking indicative of lateral spreading accompanied liquefaction at the array. Although most of the cracking appears to have been caused by local slumping along the west bank of the Alamo River toward the river, ejection of sand from some of these cracks confirms that they were associated with liquefaction. Cumulative opening across ground cracks at the array was 126 mm. The top of the inclinometer casing was deflected approximately 180 mm in a N15°E direction relative to its base beneath the liquefied layer, indicating that the upper layer slid obliquely into the north-trending Alamo River. Subsurface horizontal shear strain, estimated from the curvature of the casing, was greatest, approximately 4%, in the upper part of the silty sand.

Excess pore pressures, as recorded by the pore-pressure transducers, began to develop during the Superstition Hills earthquake when the peak horizontal ground acceleration reached 0.21g (Fig. 2) about 13.6 s after the array was triggered. The peak horizontal acceleration (0.17g) was also recorded in the downhole accelerometer beneath the silty sand at this time, which suggests that the 0.21g pulse would have been the peak acceleration at the surface even without liquefaction. Excess pore pressures were not generated either by the Elmore Ranch earthquake, which had a peak horizontal ground acceleration of 0.13g, or during the first 13.6 s of the Superstition Hills earthquake, when peak horizontal ground accelerations as large as 0.17g were recorded. Pressures throughout the entire thickness of the silty sand increased slowly following the 0.21g pulse, but at a decreasing rate, until the end of the 97-s-long record when total pore pressure approached the vertical stress caused by the total weight of the overburden, which was estimated from densities determined on soil samples (Fig. 3). Almost half of the excess pore pressure developed after 26.5 s (Figs. 2 and 3) when 90% of the earthquake shaking had propagated through the site on the basis of the measured Arias intensity (*11*) of the downhole accelerogram (Fig. 4). Thus, on the basis of the transducer measurements, liquefaction did not actually occur until after the earthquake was over.

The capacity of the silty sand layer to transmit strong motion diminished rapidly as pore pressures increased (Fig. 5). By 16 s,

Table 1. Earthquakes that triggered the Wildlife liquefaction array (*21*).

Event	Magnitude	Date (1987)	Time (PST)	Peak horizontal surface acceleration (g)
Elmore Ranch	6.2 (M)	23 Nov	1754	0.13
Aftershock	4.0 (M_L)	23 Nov	2223	0.01
Superstition Hills	6.6 (M)	24 Nov	0515	0.21
Aftershock	4.8 (M_L)	24 Nov	0535	0.02

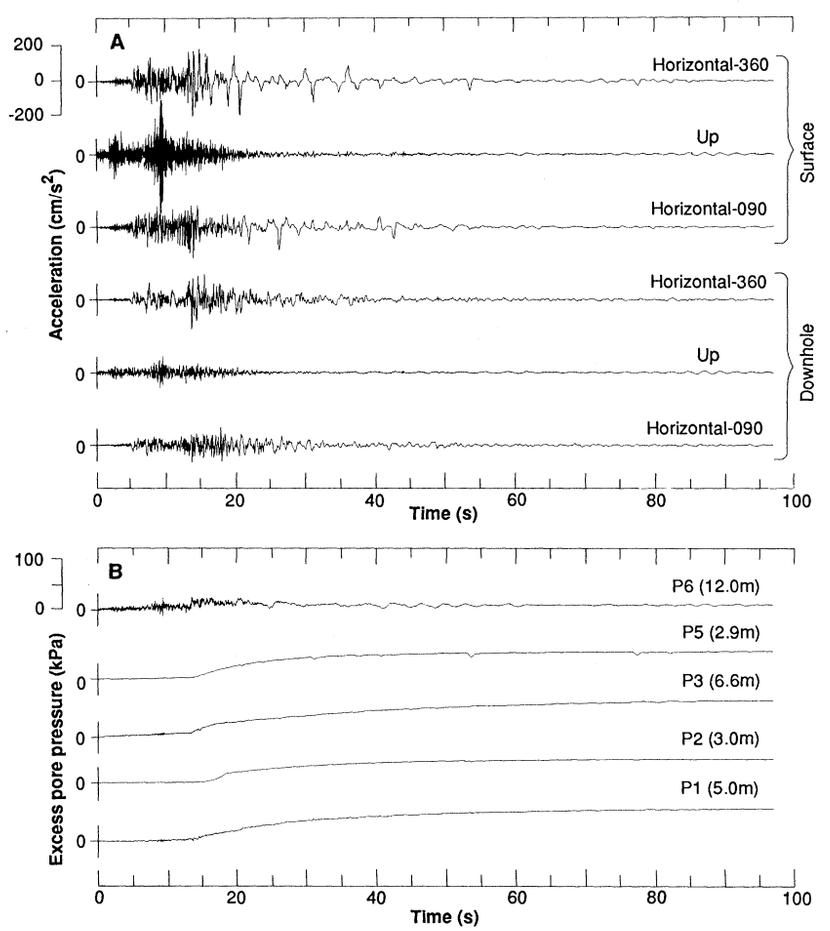

Fig. 2. Instrumental recordings from 24 November 1987 Superstition Hills earthquake. (**A**) Acceleration time histories recorded at the ground surface and beneath the liquefied layer at a depth of 7.5 m. Two horizontal components and one vertical component were recorded at both levels. (**B**) Excess pore-pressure time histories. Piezometers P1, P2, P3, and P5 are in the liquefied silty sand layer; piezometer P6 is in a silt layer that did not liquefy. Values are relative to pre-earthquake static conditions. Piezometer P4, not shown, had a large transient when it was turned on and is not believed to have functioned properly. The very small buildup of pore pressure before 13.6 s is an artifact of electrical drift of transducer output when the piezometers are turned on.

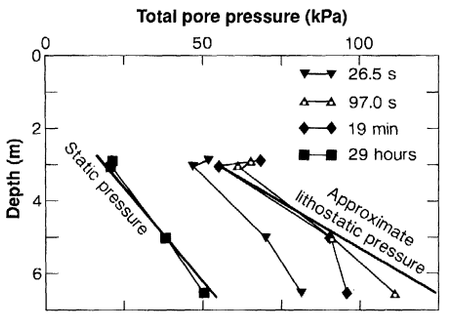

Fig. 3. Total pore pressure, static plus excess, versus depth in the silty sand layer during and after the Superstition Hills earthquake. Time is measured from instrumental trigger by earthquake. Static pore pressure is based on water table measurement. Lithostatic pressure is based on total densities of 1.6 and 2.0 g/cm^3 of overburden for above and below the water table, respectively (*22*). Approximately 90% of the earthquake shaking had propagated through the array by 26.5 s.

correlation of the surface and downhole accelerograms was extremely poor. High-frequency components of strong motion were especially degraded by excess pore-pressure generation. This degradation can be quantified by comparison of the integral of the square of acceleration with respect to time of the 360° surface accelerogram with the integral from the parallel downhole accelerometer below the silty sand layer (Fig. 4). Superposition of the integrals suggests that the silty sand started to absorb seismic energy at 13.6 s. The divergence between the two integrals continued until about 18 s.

Development of excess pore pressures immediately decreased the rigidity of the silty sand, as indicated by the doubling of the shear-wave transit time from the downhole to the surface accelerograms from 0.06 to 0.12 s at about 13.6 s (Fig. 5). This increase corresponds to a factor of 4 reduction in the average shear modulus of the 7.5-m column; the loss of rigidity of the silty sand layer must actually have been greater than this value because the silty sand occupies only 4.5 m of the 7.5-m column. We believe that a progressive loss of rigidity of the silty sand layer continued at least through 16 s (phase lags are particularly large at 14.6 s and 15.6 s), but we are less confident in correlating these phases as the coherence between the surface and downhole records degrades rapidly after 14 s.

The dynamics of the lateral spreading measured in the inclinometer casing may be expressed in the records of strong motion and pore pressure. Distinct negative pulses in the north-south (360°) surface accelerometer record at 31.2, 37.5, 40.7, 53.7, and 77.5 s correspond to transitory drops in pore pressure at 2.9 m, the depth of the shallowest transducer, P5 (Fig. 2). We suspect that these drops of pore pressure were caused by episodic lateral spreading because there are no incoming acceleration pulses on the parallel component in the downhole accelerometer, and the north-south surface accelerometer is oriented almost parallel to the N15°E slip direction recorded by the inclinometer casing.

Except for a slight decrease of pore pressure at the base of the deposit, pore pressures still supported the weight of the overburden 19 min after the Superstition Hills earthquake, when the recorder was turned on by an aftershock (Fig. 3). This local decrease in pore pressure implies that reconsolidation began as pore water was expelled (*12*) at the base of the deposit. By 29 hours after the earthquake, when we retrieved the records, excess pore pressures had completely dissipated (Fig. 3). Although water was still ponded at the site 10 hours after the Superstition Hills earthquake, when the site was first visited, no water was discharging to the surface.

The large amount of excess pore pressure that was generated after most of the earthquake strong motion ceased is surprising. Continued pore pressure generation in the absence of earthquake shaking had not been foreseen. If taken at face value, then the records imply that pore-pressure buildup during liquefaction is more complicated than is suggested by laboratory studies, which indicated that strong shaking is required to generate excess pore pressure (*2*). Although we do not preclude this possibility, we suspect that pore pressures were already lithostatic in parts of the deposit by the end of the earthquake and that the delay was caused by redistribution of pore pressures. Such pore-pressure redistribution had been anticipated in analytical investigations and observed in centrifuge tests (*13*). Independent evidence suggesting that pore pressures at the array were at least locally elevated well before 97 s includes the reduction in the shear-wave velocity, the loss of phase coherence between the uphole and downhole acceleration time histories, and the divergence until about 18 s of the record energy in the uphole and downhole accelerograms following initiation of excess pore-pressure generation at about 13.6 s.

Possible causes of the delay that involve redistribution include: (i) migration of high pore pressure from outside the instrumented silty sand layer; (ii) liquefaction of only small pockets of sediment, attributable to natural heterogeneity in the deposit; and (iii) migration of high pore pressures through nonliquefied zone around each transducer that resulted from compaction of a small zone around each transducer as it was pushed into place (*9*). The magnitude of the delay by the last mechanism depends on hydraulic diffusivity and size of the disturbed region (*14*). Any of these possibilities, or perhaps some combination of them, have important implications for either or both our understanding of liquefaction and field procedures for monitoring dynamic pore pressure.

However we come to understand the delay, the data provide direct field confirmation that pore pressures approached the vertical stress from the weight of the overburden during liquefaction, implying that vertical effective stresses and frictional strength progressed to zero. This condition developed throughout the entire 4.5-m-thick silty sand.

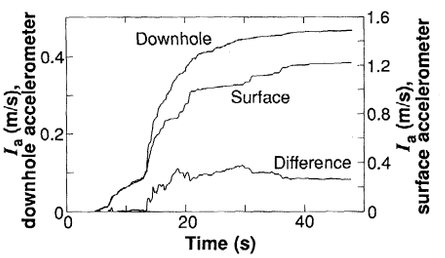

Fig. 4. Buildup of Arias intensity, I_a (*11*), as a function of time for the 360° downhole and surface accelerograms. Arias intensity for the downhole and surface accelerograms is 0.48 and 1.26 m/s, respectively. The higher surface intensity is caused by amplification effects. If amplification of the surface acceleration with respect to the downhole acceleration is linear in the absence of excess pore pressure, as we believe to be the case, then the ratio of the downhole to surface buildups before 13.6 s, 0.32, can be used to rescale the surface buildup and thereby remove the amplification effect. The difference between the downhole and rescaled surface buildups indicates the time at which the curves diverge, 13.6 s. We attribute the difference to absorption of seismic energy as excess pore pressure is generated between the two instruments.

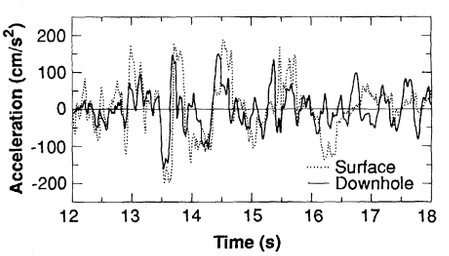

Fig. 5. Downhole and surface 360° components of acceleration from 12- to 18-s time period of the Superstition Hills earthquake that show decreasing stiffness and loss of phase coherence caused by development of excess pore pressure. Reduction in stiffness is illustrated by advancing the surface record by 0.06 s and then superimposing it over the downhole record. At about 13.6 s the downhole-to-surface travel time increases by another 0.06 s, indicating that the average shear-wave velocity between the instruments has decreased to half its original value.

Our data also support the prevailing practice in geotechnical engineering of using peak horizontal ground acceleration for predicting both liquefaction and the onset of pore-pressure increase. The absence of excess pore pressures until horizontal acceleration equaled $0.21g$ indicates that there may be a horizontal acceleration threshold for the onset of pore pressure increases. Excess pore pressures were not generated at the array during either the Elmore Ranch or the early part of the Superstition Hills earthquakes despite peak accelerations of $0.13g$ and $0.17g$, respectively. Such a threshold has been inferred from experimental and theoretical investigations (*15*).

The liquefaction response of the silty sand to both the Elmore Ranch and Superstition Hills earthquakes is successfully predicted by the method developed by Seed and colleagues (*16*). The method, which is widely used in the United States, makes use of an empirical correlation between standard penetration tests, a commonplace in situ soil engineering test (*16*), and a shear-stress parameter that is proportional to peak horizontal acceleration. Liquefaction is not predicted for the Elmore Ranch earthquake whereas liquefaction in the top and bottom of the silty sand is predicted for the Superstition Hills earthquake (Fig. 6).

These observations concerning peak acceleration are particularly relevant to the use of ancient sand boils to infer magnitudes of prehistoric earthquakes. Because peak horizontal acceleration is weakly dependent on earthquake source strength (*17, 18*), a peak acceleration constraint on liquefaction allows for a wide range of possible magnitudes of the causative earthquake. Many earthquakes with $M < 5$ have generated peak horizontal acceleration greater than $0.2g$ (*17, 19*), and many earthquakes with $M < 6$ have induced liquefaction of susceptible deposits (*20*). Both observations point to large uncertainties in estimations of magnitude from observed manifestations of liquefaction, unless the areal distribution of sand boils known to be contemporaneous can be determined accurately. Such a condition is rarely met in the study of prehistoric earthquakes, suggesting that estimating magnitudes from liquefaction evidence alone should be done with caution.

In conclusion, our in situ measurements of earthquake-induced liquefaction divulge a dynamic and complicated process with implications for paleoseismology and geotechnical engineering. The records support the concept that peak horizontal acceleration must equal or exceed a specific value for a deposit to liquefy. The value is predicted well by established methods, which permits earthquake-induced fossil sand boils to be used to infer minimum values of peak horizontal acceleration of prehistoric earthquakes, but generally not their source strength. Although the measurements confirm that pore pressures generated during liquefaction approach lithostatic, they indicate that the condition was attained after the earthquake ended. We are inclined to believe on the basis of the site response that redistribution of pore pressures caused the delay. Depending on its explanation, the delay has important implications for either or both our understanding of liquefaction and field procedures for monitoring liquefaction.

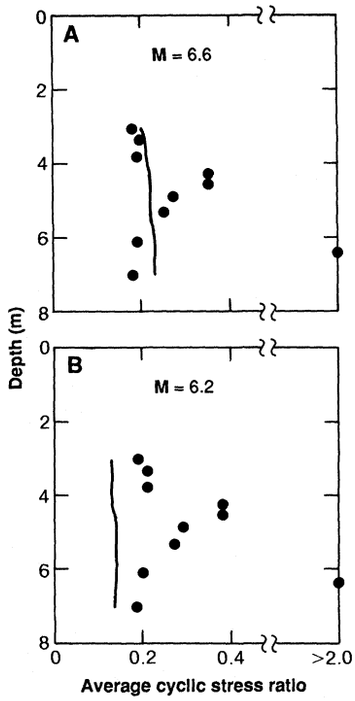

Fig. 6. Liquefaction resistance (dots) of silty sand and earthquake-induced stress (solid line) computed by the Seed method (*16*) for (**A**) Superstition Hills ($M = 6.6$) earthquake and (**B**) Elmore Ranch ($M = 6.2$) earthquake. Liquefaction is predicted when earthquake-induced stress exceeds liquefaction resistance. Average cyclic stress ratio is the ratio of average earthquake-induced horizontal shear stress to the vertical effective stress. Liquefaction is based on standard penetration tests at the array (*7*).

REFERENCES AND NOTES

1. All magnitudes are moment magnitudes unless otherwise noted [T. C. Hanks and H. Kanamori, *J. Geophys. Res.* **84**, 2348 (1979)].
2. K. Ishihara, in *Proceedings of the Eleventh International Conference on Soil Mechanics and Foundation Engineering*, San Francisco, 12 to 16 August 1985 (Balkema, Rotterdam, 1985), pp. 321–376.
3. ——, in *Proceedings of the International Conference on Recent Advances of Earthquake Engineering and Soil Dynamics*, St. Louis, 26 April to 3 May 1981, S. Prakash, Ed. (University of Missouri, Rolla, 1981), pp. 523–527; K. Ishihara, Y. Anazawa, J. Kuwano, *Soils Found.* **27**, 13 (1987); K. Ishihara, K. Shimizu, Y. Yamada, *ibid.* **21**, 85 (1981); E. L. Harp, J. Sarmiento, E. Cranswick, *Bull. Seismol. Soc. Am.* **74**, 1381 (1984).
4. K. E. Sieh, *J. Geophys. Res.* **83**, 3907 (1978).
5. S. F. Obermeier, R. E. Weems, R. B. Jacobson, G. S. Gohn, *Natl. Center Earthquake Eng. Tech. Rep. NCEER-87-0025* (1987), p. 480; S. F. Obermeier, G. S. Gohn, R. E. Weems, R. L. Gelinas, M. Rubin, *Science* **227**, 408 (1985); P. Talwani and J. Cox, *ibid.* **229**, 379 (1985).
6. T. L. Youd and G. F. Wieczorek, *U.S. Geol. Surv. Open-File Rep. 84-680* (1984).
7. M. J. Bennett *et al.*, *ibid. 84-252* (1984).
8. G. Sykes, *The Colorado Delta* (Carnegie Institution of Washington, DC, 1937).
9. Transducers are embedded in 3.8-cm-diameter cylindrical housings with a conical tip. Each transducer was emplaced by drilling a hole and then pushing the housing approximately 15 cm into the sediment.
10. J. G. Bierschwale, *Univ. Texas Geotech. Eng. Rep. GR-84-15* (1984).
11. The duration of earthquake shaking was estimated from the buildup of the integral of the square of acceleration with respect to time of the 360° cmponent of the downhole accelerometer. The integral for record duration when multiplied by $\pi/2g$ is the Arias Intensity [A. Arias, in *Seismic Design for Nuclear Power Plants*, R. Hansen, Ed. (MIT Press, Cambridge, 1969), pp. 438–483].
12. V. A. Florin and P. L. Ivanov, *Proceedings of the Fifth International Conference on Soil Mechanics and Foundation Engineering*, Paris, 17 to 21 July 1961, A. Caquot, Ed. (Dunrod, Paris, 1961), pp. 107–111; R. F. Scott, *Soils Found.* **26**, 23 (1986).
13. H. B. Seed, P. P. Martin, J. Lysmer, *J. Geotech. Eng. Div.* **102**, 323 (1976); W. D. L. Finn, written communication, 1988.
14. The potential effect of a nonliquefied zone around each transducer on pore-pressure time history was evaluated with a solution to the three-dimensional consolidation equation. We approximated the silty sand with an infinite homogeneous porous medium that was initially under hydrostatic conditions; we then instantaneously elevated the pore pressure outside a reference sphere and solved the time-dependent diffusion equation in three dimensions to compute the time history of pore pressure at the center of the sphere. Observed and theoretical results matched closely for a $c_v = 2$ cm^2/s and a spherical radius = 10 cm [for discussion see T. L. Holzer, T. L. Youd, M. J. Bennett, in *Proceedings of the Twentieth Joint Meeting of the United States–Japan Joint Panel on Wind and Seismic Effects*, Gaithersburg, MD, 17 to 20 May 1988 (National Bureau of Standards, Gaithersburg, MD, 1989)].
15. H. B. Seed, I. M. Idriss, I. Arango, *J. Geotech. Eng. Div.* **107**, 458 (1981); R. V. Whitman, *Liquefaction of Soils During Earthquakes* (National Academy of Science, Washington, DC, 1985).
16. H. B. Seed, K. Tokimatsu, L. F. Harder, R. M. Chung, *J. Geotech. Eng. Div.* **111**, 1425 (1985).
17. T. C. Hanks and D. A. Johnson, *Bull. Seismol. Soc. Am.* **66**, 959 (1976).
18. T. C. Hanks and R. K. McGuire, *ibid.* **71**, 2071 (1981).
19. L. C. Seekins and T. C. Hanks, *ibid.* **68**, 677 (1978).
20. D. K. Keefer, *Geol. Soc. Am. Bull.* **95**, 406 (1984); E. Kuribayashi and F. Tatsuoka, *Soils Found.* **15**, 81 (1975).
21. The time code on the instrumental array record for the aftershock following the Superstition Hills earthquake was incomplete; it is known only that the event was the same hour as the main shock. The most likely aftershock trigger during this 45-min interval was an $M_L = 4.8$ event at 0535 at an epicentral distance of 27 km from the array. Origin times are truncated to minutes.
22. M. Vucetic and R. Dobry, *Rennselaer Poly. Inst. Rep. CE-86* (1986).

23. We thank J. S. Sarmiento, S. Shaler, M. J. Bennett, P. V. McLaughlin, and R. L. Porcella for their efforts in establishing the liquefaction array. M. J. Bennett also provided information on the array and sediment properties. We also thank W. D. L. Finn, E. L. Harp, W. B. Joyner, D. K. Keefer, R. F. Scott, H. B. Seed, and R. V. Whitman for critical and helpful reviews of early drafts of the manuscript.

1 November 1988; accepted 30 January 1989